Monitoring of Liquid-solid two-phase pipe flow using ultrasonic pulses

Hyun Jin Park[1], Takumi Hayashi[1], Dongik Yoon[1], Yuji Tasaka[1], Yuichi Murai[1], Satoru Takano[2], and Sotaro Masanobu[3]

[1] Laboratory for Flow Control, Division of Mechanical and Aerospace Engineering, Faculty of Engineering, Hokkaido University, N13-W8, Kita-ku, Sapporo 060-8628, Japan
[2] Ocean Engineering Department, National Maritime Research Institute, 6-38-1, Mitaka, Tokyo 181-0004, Japan
[3] Offshore Advanced Technology Department, National Maritime Research Institute, 6-38-1, Mitaka, Tokyo 181-0004, Japan

Acoustic measurement using ultrasonic pulses emitted from outside the pipe wall was tried to measure a solid–liquid two-phase pipe flow. The two-phase flow is generated by adding 4 mm alumina spheres into a base liquid flow in a pipe with a 26 mm inner diameter. We emitted 4 MHz ultrasonic pulses with 4 cycles into the pipe and received echo signals reflected from solid particles. Particles were detected using a high intensity of their echo signals and their velocity was measured from the Doppler effect on the signals. Particles farther from the transducer are less detectable because particles farther from the transducer are hidden behind particles closer to the transducer. We tried to restore a particle existence probability distribution by two assumptions: linearly decreased detection rate and the statistical axial symmetry of the distribution on the measurement line. We also tried to estimate the size of particles using the phase of signals. The echoes at the solid-liquid interface and the liquid-solid interface on particles have opposite phases because of the difference in acoustic impedance of each phase. It is possible to estimate the particle size by detecting the phase-reversed pair of echoes and evaluating their time difference.

Keywords: Liquid-solid two-phase pipe flow, Particle velocity distribution, Particle size estimation, Particle existence probability distribution

1. Introduction

Energy storage and conversion technologies are essential technologies to realize a sustainable society and use energy with high efficiency. Most of them are supported by rare metals, and a stable supply of rare metals is necessary for the operation of these technologies. A huge amount of mud containing rare metals is buried in the deep seabed, and its mining is expected as one of the solutions for the stable supply [1]. The slurry [2] and airlift [3] methods have been used to continuously transport a large amount of excavated mud from the seabed to the sea surface. Since the inside of the transport pipe whose length is several kilometers long cannot be monitored, the amount of mining can only be grasped after the transportation. As a result, we know whether the mining site was appropriate only after a considerable amount of time has passed since mining in the deep sea. If it is possible to monitor solid particles near the inlet of the pipe, the amount of mining can be estimated immediately at the start of pumping and without pumping the particles to the surface.

Although already many methods for measuring liquid–solid two-phase flow have been developed and used [4], considering abrasion caused by the particles and pressure drop in the transportation pipe, an ultrasonic measurement which is non-invasive and has high durability is suitable as a monitoring method of this pipe. We have already performed ultrasonic measurements in various multiphase pipe flows, and have experience in detecting the velocity profiling in the liquid-phase from the Doppler effect contained in the echo signal and the gas-liquid interface from the intensity of the echo [5–7]. For evaluating the transport volume of mined mineral resources, first, in this paper, we try to obtain the solid phase information such as particles' size, velocity distribution and existence probability distribution, necessary for estimating the transport volume from ultrasonic echo signals.

2. Experimental facility

Fig. 1 shows a schematic diagram of the experimental facility. The facility was constructed with two vertical pipes whose diameter and length were 26 mm and about 10 m respectively, a slurry pump, a mixing tank, a particle feeder and four water jackets. The feeder continuously injected a constant supply of 4 mm size aluminum spheres near an inlet of flow pass in the tank, and this liquid–solid two-phase fluid was sucked and sent into the pipe by the pump. A net was installed inside the mixing tank to prevent the particles from circulating again and therefore only water was circulated. In the experiment, the liquid flow rate and particle volume fraction were Q_L = 6.0 m^3/s and α_S = 8%, respectively. These values were obtained by measuring the weight of each phase of the two-phase flow returning to the mixing tank in a period. Two water jackets for the ultrasonic measurement were installed at a 4 m distance on each of the updraft and downdraft pipes. A 4 MHz transducer (TDX) for emitting and receiving ultrasonic pulses, and a mirror for visually observing the flow inside the pipe were placed in each jacket. TDXs were connected with an ultrasonic pulser (JPR-600C, Japan probe) and a data logger (PicoScope 6000 series, Pico Technology). The setting parameters of these instruments are summarized in Table 1. By use of the mirror in the jacket, stereo pictures taken from two different viewing directions were obtained by a camera (HAS-L1, Ditect) working simultaneously with the data logger. Camera's frame fate was 500 fps and the difference between the two viewings was 90°.

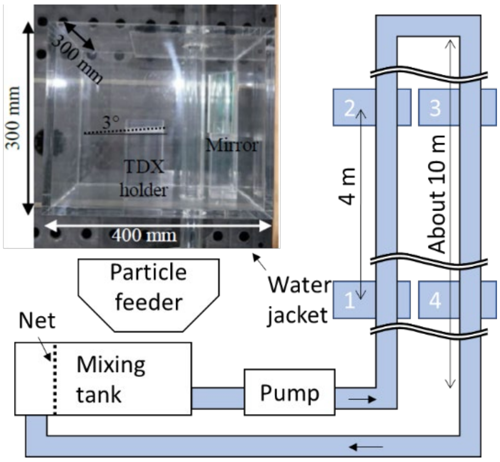

Figure 1: Schematic diagram of the experimental facility and a picture of a water jacket, where a TDX is installed with 3° to measure particle velocity in the streamwise direction and a mirror is set to take stereo pictures by a camera. The number in each jacket indicates a label of measurement points and a TDX number.

Table 1: Parameters for ultrasonic measurement

Ultrasonic pluser (JPR-600C)		
Basic frequency	4	MHz
Pulse repetition frequency	4	kHz
Cycles of pulse	4	
Emission voltage	150	V
Data logger (PicoScope 6000 series)		
Voltage range	±1 or ±2	V
Voltage resolution	8	bit
Sampling frequency	52	MHz
Recording time	5	s

3. Results and discussions

3.1 Original data: optical image and echography

Before performing the ultrasonic measurement, first, we show a sample of stereo pictures taken around TDX2 to understand the state of solid particles in the pipe flow. The alumina spheres are visualized as black circles in the picture. Although some of the particles are densely packed and appear to form clusters, they do not appear so when viewed from a 90-degree angle at the same height in the picture. It suggests that they were distributed almost randomly in the pipe and their time-averaged distribution is uniform.

Fig. 3 shows a sample of the time-space echography. The distance x on the horizontal axis in the figure is calculated by multiplying the time of flight of the ultrasonic pulse and the speed of sound in water. The pipe wall near TDX is visible on the echography at $x = 0$ mm. The opposite side wall at $x = 26$ mm, unlike the other side wall, appears to be interrupted on the time axis. This is because when many particles cross the measurement line, the ultrasonic pulse is scattered by them and weakened. When the echo intensity weakening occurs, it is confirmed that high echo intensities from the particles suddenly appear between the two walls. We extracted the echo from particles using high echo intensities over a threshold and analyzed only these echoes. A value exceeding 2σ of its average at each position on echo intensity profiles was taken as the threshold.

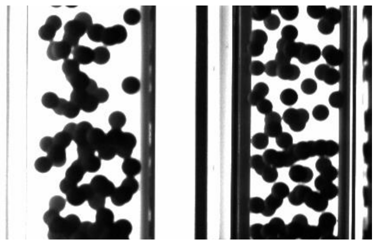

Figure 2: Sample stereo picture taken by a camera, where black circles are alumina spheres.

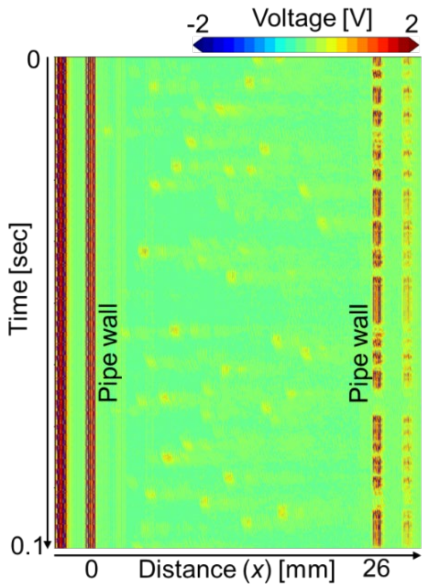

Figure 3: Sample of echography, where high amplitudes between two walls indicate alumina spheres.

3.2 Particle velocity distribution

The velocity of each particle was calculated from its echo, detected from the threshold, using quadrature demodulation [8] and autocorrelation [9]. Fig. 4 shows the average velocity distribution of the particles measured in 5 seconds. The velocity distribution is asymmetrical because the velocity in $x < 3$ mm is not measured correctly due to multiple reflections of the wall. Compared with the average particle velocities obtained from images, that obtained by the ultrasonic measurement is an appropriate result except for this region. The falling velocity of the aluminum sphere in the static water is about 0.4 m/s, but there is almost no difference in the particle velocity distribution between the updraft and downdraft pipes. And particle velocities are totally about 1 m/s lower than the bulk flow velocity of the two-phase flow in the experiment, 3.4 m/s. This difference in velocities is the slip velocity between the two phases. These results suggest that the particle velocity is mainly determined by the liquid-phase velocity and the slip velocity, regardless of the direction of flow, in the case of such a high-velocity pipe flow.

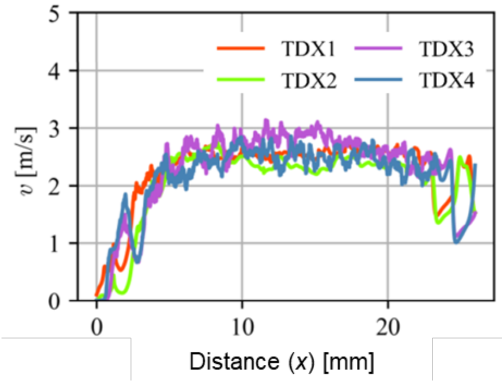

Figure 4: Average velocity distributions of particles.

3.3 Particle existence probability distribution

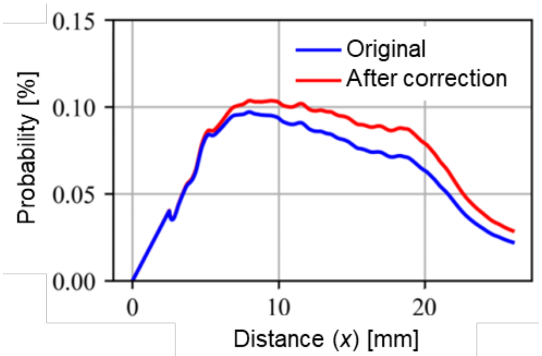

Figure 5: Particle existence probability distribution obtained from TDX2.

The blue line in Fig. 5 shows the ratio of the time when the echo from the particle is detected using the threshold during the measurement time for each position. Note that particle detection in $x < 3$ mm was not performed correctly due to multiple reflections and, therefore, linear interpolation was performed in this region as the zero probability of particle existence at the wall. In ultrasonic measurement, generally, the echo intensity from the particle becomes weaker as the distance from TDX increases. It is caused by the attenuation of the ultrasonic pulse in the medium and the reflection of the pulse by the particles on the front side. Even if the particle existence distribution is the same at all positions, the probability of particle detection decreases as the distance from the TDX increases due to the reasons described above. Therefore, a kind of correction is necessary to obtain the actual particle existence probability from the echography. We used two assumptions for the correction. One is that the probability of particle detection failure increases constantly with the distance from TDX. The other is that the existence distribution of particles is symmetrical with respect to the axis of the pipe. The red line in the figure shows the result of correction using these assumptions and the echography. The corrected distribution is flatter than the existing distribution near the axis of the pipe. And since the values in this region are similar to $\alpha_S = 8\%$, it is supposed that this method is overall effective. However, the asymmetry still remains in spite of the correction. The reason of this is that the effect of multiple reflections near the wall could not be eliminated in the preprocessing, and the existence probability of particles near the wall decreased sharply.

3.4 Particle size distribution

Focusing on the particle echo in the echography as Fig. 6(a), we can find two echoes from one particle on one ultrasonic pulse emission. This is because the ultrasonic pulse was reflected at the front and back interfaces of the particle, respectively. What is interesting about these two echoes is that their phases are reversed as shown in Fig. 6(b), where C_C is the calculated value of the cross-correlation between the emitted ultrasonic pulse and each echo. When acoustic waves move from a medium with high acoustic impedance to a medium with low acoustic impedance, the phase of echo reflected at the interface is reversed because of a negative reflection rate $R < 0$ at the interface as shown in (c). In the opposite case, i.e. when a sound wave moves from a medium with a low acoustic impedance to a medium with a high acoustic impedance, the echo from their interface has the same phase as the Incident wave. Since the acoustic impedance of aluminum is higher than that of water, the echo from the back interface has the reversed phase and its C_C is negative.

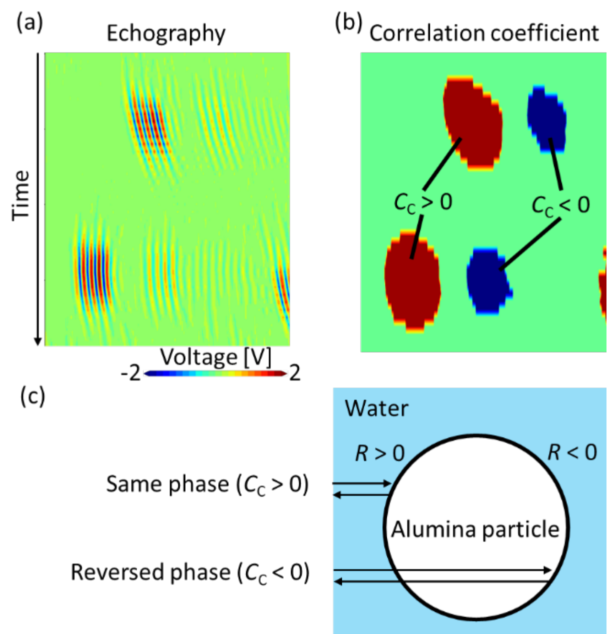

Figure 6: (a) echography zooming up near the echoes from particles, (b) cross-correlation between the emitted ultrasonic pulse and each echo, where values are ternarized, and (c) illustration of why one particle produces two echoes with different phases.

Fig. 7(a) shows a method to estimate each particle's diameter d. It is founded on the longest time interval between the start times of the phase-reversed pair Δt for the estimation. In this experiment, since we already know the material of all particles is alumina, the particle diameter is possible to calculate from time interval by multiplying the speed of sound in alumina, i.e., $d = c_A \Delta t$. The distribution of particle diameter obtained from the estimation is shown in Fig. 7(b). Since phase-reversal pairs were not detected in all particles, the particle size distribution is shown here only for those in which pairs were detected. Although all particles injected in the fluid have actually the same diameter, 4 mm, the range of estimated diameters is in $d \leq 6$ mm. First, smaller diameters than 4 mm are caused by two reasons. One is that the center of the particle does not always pass through the axis of the measurement line. The effective diameter of the TDX used in this experiment is 5 mm, and if the particle's center passes within 4.5 mm from the axis, the particle is detected and its diameter is estimated. In principle, the particle diameter is estimated by this estimation method to be smaller as the particle center is farther from the axis. The reason for the overestimated particle diameter, i.e., $d > 4$ mm, is under investigation and a clear explanation cannot be given at this time. This underestimation is expected to reduce using statistics if we can grasp what kind of diameter distribution appears for a single particle size [10]. Since the cause of the overestimation is unknown, it is necessary to investigate the cause and the correction method in the future. Even though over- and under-estimations exist in this method, it is possible to grasp the order of particle size.

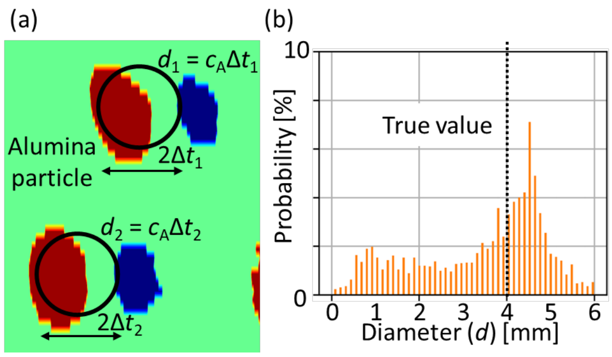

Figure 7: (a) a method to estimate a particle diameter and (b) a distribution of the estimated particle diameter.

Summary

In this paper, for the purpose of estimating the solid-phase flow rate in a solid–liquid two-phase pipe flow by the ultrasonic pulse echography, we tried to obtain solid phase information necessary for flow rate estimation from the echography. The information that was successfully acquired is the average advection velocity distribution, existence probability distribution and diameter distribution of the solid particles. First, only the echoes from the particles were extracted in the echography using a threshold for the echo intensity and we analyzed only those echoes. The particle velocities were calculated from the Doppler effect contained in the echoes. Although the flow velocity near the pipe wall could not be obtained due to multiple reflections on the wall, reasonable flow velocity distribution was obtained in the other region. Also, when obtaining the existence probability distribution of particles, the probability of detecting particles far from the transducer decreases due to shadows of particles located near the transducer. To prevent this decrease, the distribution was corrected by assuming that the decrease occurs more in proportion to the distance and that the distribution is symmetrical to the pipe axis. The particle existence probability near the wall was lost due to the multiple reflection mentioned when obtaining the velocity distribution, and therefore it was not possible to correct it to be axially symmetrical. In spite of this asymmetricity of the corrected distribution, since the existence probability obtained near the pipe center and the particle volume fraction given as the initial condition were almost the same. From this, it suggests that this measurement method is effective although there is a problem with the accuracy. The last, for particles whose front and back interfaces were detected in the echography, the diameter of each particle was calculated using the time of flight and speed of sound inside the particle. The measured diameter was obtained as a distribution from 0 to 1.5 times the actual diameter, and the peak in the diameter distribution appeared at a 13% larger diameter than the actual diameter. It means that this method can roughly estimate the particle diameter.

Acknowledgment

This work was supported by JSPS KAKENHI Grant No. JP21H04590.

References

[1] Hein J, *et al.*: Deep-ocean mineral deposits as a source of critical metals for high- and green-technology applications: comparison with land-based resources, Ore Geol. Rev., 51 (2013), 1–14.
[2] Wang R, *et al.*: Slurry pumps in deep-sea mining: A review of numerical and experimental studies, Ocean Eng., 251 (2022), 111150.
[3] Shimizu K & Takagi S: Study on the performance of a 200 m airlift pump for water and highly-viscous shear-thinning slurry, Int. J. Multiphase Flow, 142 (2021), 103726.
[4] Oddie G & Pearson JRA: Flow-rate measurement in two-phase flow, Annu. Rev. Fluid Mech., 36 (2004), 149–172.
[5] Hitomi J, *et al.*: Ultrasound Flow-monitoring and flow-metering of air–oil–water three-layer pipe flows, IEEE Access, 5 (2017), 15021–15029.
[6] Murai Y, *et al.*: Ultrasound Doppler measurement of air-lift two-phase and particulate three-phase pipe flows, Exp. Fluids, 63 (2022), 126.
[7] Yoon D, *et al.*: Ultrasound measurement of large bubbles rising in angled slug pipe flows, Flow Meas. Intrum., 91 (2023), 102357.
[8] Murakawa H, *et al.*: Effects of the number of pulse repetitions and noise on the velocity data from the ultrasonic pulsed Doppler method with different algorithms, Flow Meas. Instrum., 40 (2014), 9–18.
[9] Kasai C, *et al.*: Real-time two-dimensional blood flow imaging using an autocorrelation technique, IEEE Trans. Sonics Ultrasonics, 32 (1985), 458–464.
[10] Park HJ, *et al.*: Spatial development of single void pulse in a horizontal turbulent bubbly channel flow investigated by a time-resolved two-laser measurement, int. J. Multiphase Flow, 146 (2022), 103867.